Thermal Imagery Based Instance Segmentation for Energy Audit Applications in Buildings

Youness Arjoune[1], Sai Peri[1], Niroop Sugunaraj[1], Debanjan Sadhukhan[1], Michael Nord[2], Gautham Krishnamoorthy[3], David Flynn[4], and Prakash Ranganathan[1]

***Abstract*—Energy audit in buildings is an essential task for optimal energy management and operations. This paper focuses on a machine learning pipeline to quantify heat loss using 60,000 thermal images in buildings. The images are captured from a small Unmanned Aerial System (sUAS) over the last two years to form a large thermal data repository. Intense efforts are made to annotate multiple sections of the buildings (e.g. windows, doors, ground, facade, trees, and sky). Data augmentation processes are then applied to generate a large comprehensive training data set. Object detection and instance segmentation models such as Mask R-CNN, Fast R-CNN, and Faster R-CNN were trained, and tested. The preliminary results indicate that Mask R-CNN has a larger mean average precision (mAP) of (83%) over R-CNN (51%), Fast R-CNN (62%), and Faster R-CNN (62 %) for a threshold of 50%. The surface temperature values from these thermal images (pixel-by-pixel) were then used in the standard heat transfer coefficient (U-value in BTU/hr/Sq.ft./F) calculations.**

***Index Terms*—Heat Loss, Mask R-CNN, mAP**

I. Introduction

Thermal performance assessment of building(s) is a key process for energy management operations in heat loss evaluation. Identifying various sections of buildings for thermal anomalies may help to foresee various retrofit interventions and lower maintenance costs or operations. Affordable Infrared (IR) cameras mounted on an Unmanned Aerial Vehicle (UAV) provides an alternative method to quantify heat loss. Thermal anomalies represent the number of thermal imperfections present in the investigated object [1]–[3]. One way of performing the quantitative assessment of a building is by providing the overall thermal transmittance of different parts of the buildings, generally known as the "U-value". The U-value is defined as the rate of heat that flows through one square meter of the wall (or the inspected part of the wall) from/to the outside air when the temperature difference between the inside and outside is one Kelvin under steady state conditions. The unit of U-value is $BTU/ft^2/hr/F$ or $Wm^{-2}K^{-1}$. In our analysis, we discard certain sections of images (such as the sky, the ground around the building face, or trees) using an instance segmentation process, and considered them as noise as they can result inaccurate U-value/heat-loss calculation. We only use objects such as windows, doors, and walls to estimate the U-values from these thermal images [4], [5].

II. Literature Review

Several machine learning based methods for object detection such as Region-based Convolutional Neural Network (R-CNN), Fast R-CNN, Faster R-CNN, and Mask R-CNN were proposed in [6]–[8]. In R-CNN, a finite and manageable number of bounding boxes are identified for Regions of Interest (RoIs), and CNN features are extracted for each boxes independently for classification. The Fast R-CNN and Faster R-CNN models unify independent models into a single efficient model. The authors of [9]–[11] use these models for various applications such as face detection, human organ segmentation, and vehicle detection.

The overall thermal performance of the buildings can be estimated via two type of measurements: 1) qualitative and 2) quantitative measurements. In qualitative measurements, various sections of the buildings are identified only when *thermal bridging* is observed. A *thermal bridge* is an area or a component of an element that shows a larger heat flow than the surrounding elements. The quantification of thermal loss is not required in such measurement type. Various techniques to evaluate the overall heat transmittance of the buildings have been reported in literature [12]–[17].

III. Methodology

A. Data Collection

Using a sUAS equipped with a FLIR camera, and with partnerships with a local UAS company (SkySkopes Inc.) in North Dakota, hundreds of infrared images were taken. A guideline to acquire thermal images from buildings were developed, and followed strictly to adhere consistency in the acquisition of images. Prior to data collection, a piece of aluminum foil and black tape were placed on each building to calculate the reflected temperature and emissivity. A HOBO sensor was placed inside each building being photographed to measure the other weather variable (e.g., temperature) inside the buildings.

Temperature data from the images is extracted using FLIR software. This data is then used to calculate the temperature on the aluminum foil and black tape, and the wall temperature. The temperature of the aluminum foil is used to calculate the reflective temperature and the temperature of the black tape is used to calculate the emissivity [18]. The outdoor temperature is obtained from the HOBO sensor that accompanied the drone and the wind speed measurements are obtained from weather data.

B. Data Training

A machine learning pipeline for our thermal data repository is developed and shown in Fig. 1. A collection of

978-1-7281-0858-2/19/$31.00 © 2019 IEEE
978-1-7281-0858-2/19/$31.00 ©2019 IEEE

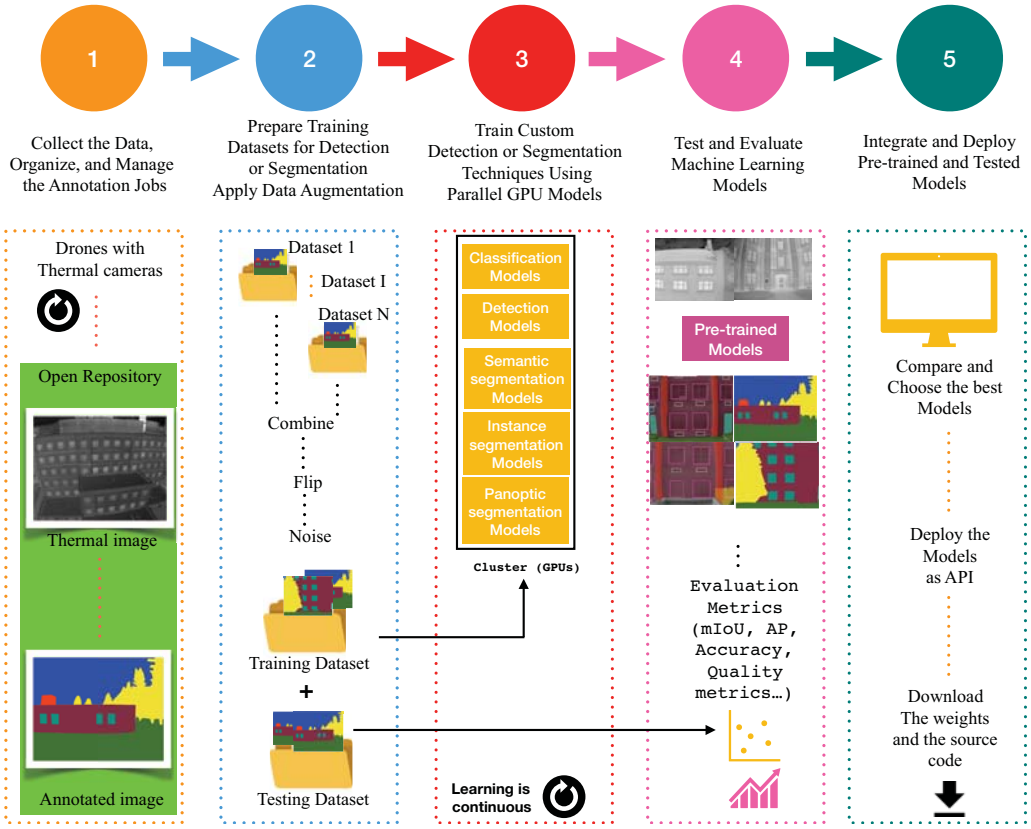

Fig. 1. Machine Learning Pipeline for Building Audits

thermal images (approx. 2.5k images per building) are captured by SkySkopes using ZENMUSE XT Radiometruc FLIR 640X512(30 Hz) and OGI sensors. Gray-scale images are converted to pseudo color images (using iron-bow filter) for annotation (with data augmentation of x10) and split into training (70%) and testing (30%). Our data repository includes thermal images, historical weather, building material, and cost variables that span across multi-years crossing several TeraBytes (TB) of data becoming a Big Data problem. Typically, in order to handle such large amounts of data, high performance computers need to be deployed. Specifically, the instance segmentation techniques in this paper are trained with learning rate of 0.001 on a 4-GPUs node High Performance Computing (HPC) environment. The segmented images are then used to estimate the U-values (Eq. 1) for heat loss quantification [18].

$$U = \frac{\sigma\epsilon(T_s^4 - T_{ae}^4) + 3.805v(T_s - T_{ae})}{T_{ai} - T_{ae}} \quad (1)$$

where σ stands for the Stefan-Boltzmann constant, ϵ stands for emissivity, T_s denotes the surface temperature, T_{ae} denotes the external air temperature, v denotes the wind velocity, and T_{ai} denotes internal air temperature.

IV. Results and Discussions

To evaluate the object detection and instance segmentation methods, performance metrics such as mean Average Precision (mAP) and mean Intersection over Union ($mIoU$) are used. The precision (AP) measures the percentage of correct predictions using the following equation:

$$Precision = \frac{TP}{TP + FP} \quad (2)$$

where TP and FP denotes true positives and false positives respectively. AP is defined as average on the precision of classes, and mAP is the average on AP. IoU measures the number of pixels that are common between the target and prediction masks. The IoU is defined as

$$IoU = \frac{\text{Area of overlap}}{\text{Area of union}} \quad (3)$$

If the IoU is greater than a certain threshold, it is treated as TP, otherwise it is a FN. mean IoU ($mIoU$) is defined as the average on IoU. The $mAPs$ and $mIoUs$ values for R-CNN, Faster R-CNN with different kernels/data set, and Mask R-CNN are shown in Table I. $AP^{0.5}$ denotes if the IoU is greater than 50%, then the detection is considered to be TP, otherwise FP. The results of our preliminary findings are summarized in Tables I and II. Table I show the results of R-CNN, Fast R-CNN, Faster R-CNN, and Mask R-CNN. The results indicate that Mask R-CNN produces a better accuracy over Fast and Faster R-CNN. The actual $mAP^{0.5}$ using Mask R-CNN for each object are as follows: Windows (80%), Facades (89%), and Trees (80%). In our analysis, Mask R-CNN achieves

Training/Testing Results of Convolution Algorithms				
Models	$mAP^{0.25}$	$mAP^{0.5}$	$mAP^{0.75}$	$mIoU$
RCNN	0.53	0.51	0.32	0.76
Faster RCNN	0.68	0.62	0.40	0.82
Faster RCNN ResNet 50	0.83	0.58	0.53	0.75
Faster RCNN Inception ResNetV2	0.65	0.62	0.51	0.83
Mask R-CNN	0.83	0.83	0.59	0.80

TABLE I: mAP values for Instance segmentation methods

Average U-value ($BTU/ft^2/hr/F$)						
Building Name	**Wall** Sample 1	**Wall** Sample 2	**Wall** Sample 3	**Windows** (Face 1)	**Windows** (Face 2)	**Windows** (Face 3)
Twamley Hall	0.005	0.02	0.02	1.14	0.7	0.6
Museum	0.07	0.08	0.06	0.3	0.28	0.4

TABLE II: U-values for Twamley and ND Musuem of Art Buildings

overall mAP of 83% for $mAP^{0.5}$. It is important to note that the training time of mask R-CNN on 4-GPU is only 1.88 seconds per image with a size of 512x640.

Table II show the overall U-values (using Eq. 1) for different faces (or walls) and windows of two buildings (e.g.Twamley and ND Museum of Art). It is observed that the U-values for windows in Twamley are larger than ND Museum. This is an anticipated result as the windows in Twamley are older and are of single pane type, while the windows in Museum building are new and upgraded with double pane types. It is desired to have a lower U-value for heat loss quantification.

V. Conclusion

A machine learning workflow for energy audit in buildings is presented. A collection of 60000 thermal images were analyzed by object detection and instance segmentation techniques such as Fast R-CNN, Faster R-CNN, and Mask R-CNN. The preliminary findings indicate Mask R-CNN produces better mAP of (83.0%) in segmenting objects for thermal imagery. The heat loss co-efficient (U values) are then quantified using extracted surface temperatures with other weather variables.

VI. Acknowledgement

The authors acknowledges the support received from the North Dakota Department of Commerce grant (Research ND award # UND22166). We also thank our collaborator Mr. Matt Dunlevy (CEO of SkySkopes Inc, Grand Forks, ND, USA) for his assistance in acquiring a collection of a large thermal image dataset.

References

[1] E. Lucchi, "Applications of the infrared thermography in the energy audit of buildings: A review," *Renewable and Sustainable Energy Reviews*, vol. 82, pp. 3077–3090, 2018.

[2] B. M. Marino, N. Muñoz, and L. P. Thomas, "Estimation of the surface thermal resistances and heat loss by conduction using thermography," *Applied Thermal Engineering*, vol. 114, pp. 1213–1221, 2017.

[3] "Residential energy services network (resnet). interim guidelines for thermographic inspections of buildings. resnet," 2012.

[4] K. Koiner, A. Rosener, D. Sadhukhan, D. F. Selvaraj, Z. E. Mrabet, M. Dunlevy, and P. Ranganathan, "Heat loss estimation using uas thermal imagery," in *IEEE EIT 2019*. IEEE, 2019.

[5] K. He, G. Gkioxari, P. Dollár, and R. Girshick, "Mask r-cnn," in *Proceedings of the IEEE international conference on computer vision*, 2017, pp. 2961–2969.

[6] R. Girshick, "Fast r-cnn," in *The IEEE International Conference on Computer Vision (ICCV)*, December 2015.

[7] K. He, G. Gkioxari, P. Dollar, and R. Girshick, "Mask r-cnn," in *The IEEE International Conference on Computer Vision (ICCV)*, Oct 2017.

[8] S. Ren, K. He, R. Girshick, and J. Sun, "Faster r-cnn: Towards real-time object detection with region proposal networks," in *Advances in neural information processing systems*, 2015, pp. 91–99.

[9] H. Jiang and E. Learned-Miller, "Face detection with the faster r-cnn," in *2017 12th IEEE International Conference on Automatic Face & Gesture Recognition (FG 2017)*. IEEE, 2017, pp. 650–657.

[10] C. Chen, L. Ma, Y. Jia, and P. Zuo, "Kidney and tumor segmentation using modified 3d mask rcnn," 2019.

[11] Q. Fan, L. Brown, and J. Smith, "A closer look at faster r-cnn for vehicle detection," in *2016 IEEE intelligent vehicles symposium (IV)*. IEEE, 2016, pp. 124–129.

[12] A. Donatelli, P. Aversa, and V. A. M. Luprano, "Set up of an experimental procedure for the measurement of thermal transmittances via infrared thermography on lab made prototype walls," *Infrared Physics & Technology*, vol. 79, pp. 135–143, 2016.

[13] B. Tejedor, M. Casals, M. Gangolells, and X. Roca, "Quantitative internal infrared thermography for determining in situ thermal behaviour of façades," *Energy and Buildings*, vol. 151, pp. 187–197, 2017.

[14] M. OGrady, A. A. Lechowska, and A. M. Harte, "Quantification of heat losses through building envelope thermal bridges influenced by wind velocity using the outdoor infrared thermography technique," *Applied energy*, vol. 208, pp. 1038–1052, 2017.

[15] M. O'Grady, A. A. Lechowska, and A. M. Harte, "Infrared thermography technique as an in situ method of assessing heat loss through thermal bridging," *Energy and Buildings*, vol. 135, pp. 20–32, 2017.

[16] G. Baldinelli, F. Bianchi, A. Rotili, D. Costarelli, M. Seracini, G. Vinti, F. Asdrubali, and L. Evangelisti, "A model for the improvement of thermal bridges quantitative assessment by infrared thermography," *Applied energy*, vol. 211, pp. 854–864, 2018.

[17] A. Marshall, J. Francou, R. Fitton, W. Swan, J. Owen, and M. Benjaber, "Variations in the u value measurement of a whole dwelling using infrared thermography under controlled conditions," *Buildings*, vol. 8, no. 3, p. 46, 2018.

[18] I. Nardi, D. Paoletti, D. Ambrosini, T. De Rubeis, and S. Sfarra, "U value assessment by infrared thermography: A comparison of different calculation methods in a guarded hot box," *Energy and Buildings*, vol. 122, pp. 211–221, 2016.